599696

Variations in the Strength of the Infrared Forbidden 2328.2 cm^{-1} Fundamental of Solid N_2 in Binary Mixtures

by

Max P. Bernstein and Scott A. Sandford

NASA-Ames Research Center, Astrophysics Branch,

Mail Stop 245-6, Moffett Field, California 94035-1000

Submitted to *Spectrochimica Acta, Part A, Molecular Spectroscopy*

Submitted: _____

Received: _____

21 Pages (excluding Figures)

5 Figures

2 Tables

Correspondence Author's Contact Information:

Dr. Max P. Bernstein
NASA-Ames Research Center
Mail Stop 245-6
Moffett Field, CA 94035-1000
Phone: (650) 604-0194
Fax: (650) 604-6779
Email: mbernstein@mail.arc.nasa.gov

Abstract

We present the 2335-2325 cm^{-1} infrared spectra and band positions, profiles, and strengths (*A* values) of solid nitrogen and binary mixtures of N_2 with other molecules at 12 K. The data demonstrate that the strength of the infrared forbidden N_2 fundamental near 2328 cm^{-1} is moderately enhanced in the presence of NH_3, strongly enhanced in the presence of H_2O and very strongly enhanced in the presence of CO_2, but is not significantly affected by CO, CH_4, or O_2. The mechanisms for the enhancements in N_2-NH_3 and N_2-H_2O mixtures are fundamentally different from those proposed for N_2-CO_2 mixtures. In the first case, interactions involving hydrogen-bonding are likely the cause. In the latter, a resonant exchange between the N_2 stretching fundamental and the $^{18}O{=}^{12}C$ asymmetric stretch of $^{18}O^{12}C^{16}O$ is indicated. The implications of these results for several astrophysical issues are briefly discussed.

Key Words: Nitrogen; Carbon dioxide; Water; Infrared Spectroscopy; Interstellar Ices; Matrix Isolation

1. Introduction

While infrared forbidden in the gas phase, the N_2 fundamental stretching vibration near 2328 cm^{-1} can be perturbed into infrared activity in the solid state through interactions with neighboring species. The nature of this interaction has received considerable attention over the years and has been studied in pure N_2 ices [1-4] and in a number of N_2-containing ice mixtures [5-11]. This earlier work, combined with the realization that N_2-rich mixed-molecular ices are present in the outer solar system [12] and probably in cold, dense clouds of dust, gas, and ice in the interstellar medium [13], have led us to conduct a laboratory study on the variation in the absorption intensity of the infrared forbidden N≡N fundamental stretch near 2328 cm^{-1}.

The methods and materials used in this study are described in the following section (§2). In §3 we present spectra of the 2328 cm^{-1} N≡N stretching band produced by N_2 in a variety of binary ice mixtures, and examine the change of this feature's intensity as a function of the identity and concentration of the second molecule. A discussion of the results of the work is provided in §4, and §5 contains some brief comments on the implications of this work for several astrophysical issues. Our findings are summarized in §6.

2. Materials and Methods

The techniques and equipment employed for this study have been described in detail as part of our previous studies of mixed-molecular ices [13-15]. Details associated with the materials and methods used that are unique to this particular study are provided below.

2.1 Starting Materials

The N_2 gas used (Airco, 99.95%) was further purified by passing it through a liquid nitrogen-cooled trap to remove condensable contaminants prior to mixing with other gases. Most of the other gases used in our experiments, $^{15}N_2$ (Aldrich, 98.0%), $^{13}CO_2$ (Aldrich, 99.0%), CO_2 (Matheson, 99.8%), CH_4 (Matheson, 99.99%), O_2 (Matheson, 99.99%), NH_3 (Matheson, 99.99%), and CO (Matheson, 99.99%), were taken directly from lecture bottles without further purification. Distilled H_2O was further purified by three freeze-pump-thaw cycles under vacuum ($P<10^{-5}$ mbar) prior to mixing in order to remove dissolved gases.

2.2 Sample Preparation

All the compounds had sufficient volatility at room temperature that samples could be prepared by mixing, in the gas phase, appropriate amounts of N_2 with the compound of interest. The relative gas abundances were controlled using a greaseless glass gas-handling system described elsewhere [14] and the gases were mixed in volume-calibrated, greaseless glass bulbs. All bulbs were mixed at room temperature and allowed to equilibrate for at least 24 hours before use. The background pressure in the gas-handling system was ~10^{-6} mbar. The total pressure in the sample bulbs varied

depending on the relative concentration of N_2 to the second gas and its identity, but the sample bulbs never contained less than 20, or more than 1000, mbar of total pressure. Thus, the contaminant levels in the bulbs associated with the mixing process are always less than about one part in 10^7, i.e., are negligible compared to the original impurities of our starting materials.

Once prepared, glass sample bulbs were transferred to the stainless steel vacuum manifold where the sample mixture was vapor-deposited onto a CsI window cooled to 12 K by an Air Products Displex CSW 202 closed-cycle helium refrigerator. Typical samples were deposited at a rate of about 1.0 mmole/hour, corresponding to an ice growth rate of approximately 5 μm/hour. Under these conditions, N_2-rich ices are expected to be in the α structural form.

2.3 Determination of N_2 Band Strengths

Infrared spectra were obtained from the condensed samples using a Nicolet 7100 Fourier transform spectrometer at a resolution of 0.9 cm^{-1} (the width of an unresolved line) and normalized by ratioing to a spectrum of the blank cold finger obtained prior to gas deposition. The intrinsic strength, A, of any bands of interest in the spectra were determined by measuring the integrated area of the band in absorbance and dividing by the column density of the molecule responsible, i.e.,

$$A = \int \tau(\nu)\, d\nu \,/\, N \qquad (1)$$

where $\tau(\nu)$ is the frequency dependent optical depth across the absorption feature, ν is the frequency in cm^{-1}, and N is the column density in molecules/cm^2. The intrinsic strength is then given in units of cm/molecule.

In this work, the A values for the N≡N stretching vibration near 2328 cm^{-1} produced by N_2 in different ice mixtures were determined using two independent methods. In the first, we scaled the area of the N_2 band at 2328 cm^{-1} to that of a known absorption band produced by the other molecule in the ice. Using the known relative concentration of the N_2 and the second molecule, and the known A value of the band produced by the second molecule, it was then a simple matter to derive the A value for the N_2 by scaling. The derivation of A_{N2} using this method did not require a direct measurement of the actual column densities of the materials in the measured sample but was only as accurate as the A value used for the strength of the band of the second molecule.

In this paper, we use the following A values: A_{CO}(2140 cm^{-1} band) = $1.0x10^{-17}$ cm/molecule, A_{CO2}(2344 cm^{-1} band) = $1.4x10^{-16}$ cm/molecule, A_{CH4}(1301 cm^{-1} band) = $3.8x10^{-18}$ cm/molecule, A_{NH3}(1070 cm^{-1} band) = $1.7x10^{-17}$ cm/molecule, and A_{H2O}(1660 cm^{-1} band) = $1.4x10^{-16}$ cm/molecule. These are based on A values measured for these molecules in similar ice mixtures [16,17], and are expected to involve uncertainties of no more than a factor of about 50%. In some of our thicker N_2:CO_2 ices the 2344 cm^{-1} $^{12}CO_2$ band was saturated and could not be measured. In these cases, we integrated the strength of the weaker $^{13}CO_2$ band and scaled by the $^{12}CO_2/^{13}CO_2$ band strength ratios measured from thinner samples where the $^{12}CO_2$ band near 2344 cm^{-1} was not saturated.

For the second method, we used interference fringes formed in the baseline of the infrared spectrum by multiple reflections of the infrared beam within the solid sample film to determine a sample thickness and then derived the column density of the sample using an assumed index of refraction and density of the sample. The A value for the N_2 fundamental was then determined by dividing the integrated area of the N_2 absorption band by the column density of N_2. For this method we generally assumed the samples had an index of refraction of 1.23 (that of pure N_2) [18] and densities of 1.0271 g/cm^3 [19]. The values of these two parameters undoubtedly differ slightly from sample to sample, especially for those with high concentrations of guest molecules, but with the exception of H_2O as a guest molecule, these effects are expected to result in uncertainties of less than a few percent. Since pure H_2O ice has a significantly higher index of refraction than N_2, we used the relative concentrations of N_2 and H_2O in our N_2-H_2O samples to interpolate an index of refraction between the value of 1.23 for pure N_2 and a value of 1.32 for pure H_2O [16]. Overall, for those samples that produced good interference fringes in their spectra, this technique results in final N_2 A values having uncertainties of 25% at most.

It was necessary to use both of these methods because neither method could be applied to all of the ice mixtures examined. For example, it was not possible to use the interference fringe technique for samples where the ice contained large concentrations of H_2O since this molecule produces a number of strong and broad bands that mask the fringes. Similarly, the technique of ratioing band

areas requires prior information about the intrinsic strengths of bands produced by the second molecule in the mix, information that is not available for all the mixes and concentrations studied here. Nonetheless, we are confident that both techniques provided reliable results within better than a factor of three since (i) when both techniques could be used on the same sample, they yielded strengths that always agreed to better than a factor of three (typically better than a factor of 1.5-2.0) and both yielded identical trends and (ii) both techniques yielded values for our samples with high N_2 concentrations that agree with those already published for high concentration N_2 ices [20].

3. Results

3.1 The Position and Profile of the Nitrogen Fundamental

Since the N_2 stretching fundamental is only seen in ices because interactions with neighboring molecules lead to symmetry breaking, it would not be surprising if the position and profile of this feature were a function of the samples' composition. Fig. 1 presents the 2338-2322 cm^{-1} (4.277-4.307 μm) infrared spectra of six N_2-rich ices deposited and maintained at 12 K. The top spectrum is that of pure N_2; the N≡N stretch produces an absorption band centered at 2328.2 cm^{-1} (4.2952 μm) with a full-width-at-half-maximum (FWHM) of ~1.5 cm^{-1} (0.0028 μm). As can be seen from Fig. 1, the addition of ~5% CO, CH_4, O_2, or NH_3 has little affect on the position or profile of the N_2 stretching band, although the presence of NH_3 does cause the band to broaden slightly. Nitrogen ices containing 5% H_2O produce an N_2 band that is about twice as broad as the other ices.

The presence of CO_2 does not produce a wider N_2 band. However, in addition to the N≡N stretching band, the 2338-2322 cm^{-1} spectra of N_2-CO_2 ices contain a second band at 2332.0 cm^{-1} (4.2882 μm). The 2332.0 cm^{-1} band is interpreted as being due to the ^{18}O isotopic band of the CO_2 asymmetric C=O stretching mode [5-8]. Fig. 2 presents the 2338-2322 cm^{-1} (4.277-4.307 μm) infrared spectra of a number of 12 K N_2-rich ices containing CO_2 in concentrations ranging from 1 part in 400 up to 1 part in 2. Note that the N_2 band near 2328 cm^{-1} and the $^{18}O^{12}C^{16}O$ band near 2332 cm^{-1} have similar strengths over most of this range of relative concentrations. This peculiar behavior will be discussed in more detail in §3.2 and §4.2.2.

The positions, widths, and strengths of the N≡N stretching band of the N_2-rich ice mixtures shown in Fig. 1 are summarized in Table I. The interpretation of the infrared and Raman positions and profiles of the N_2 fundamental and of the bands of molecules interacting with N_2 has received substantial attention over the years. For considerably more detailed discussions of these interactions, the reader is encouraged to see references 1-10.

3.2 Changes in the Intrinsic Strength of the N_2 Fundamental

Since the N_2 stretching fundamental is classically infrared forbidden, its absolute strength in solids is, not surprisingly, a strong function of composition. Indeed, it was the observation that the N_2 fundamental becomes 'infrared active' in the presence of CO_2 [5,6] that stimulated much of the early work on this band. Subsequent observations of the N_2 band enhancement in the presence of CO_2 [3,7,8] were extended to include other guest molecules including HF, DF, HCL, and DCl [10], ICN and BrCN [9], C_2N_2 [7,9], and H_2O and D_2O [7,9,10]. This earlier work was largely confined to issues associated with the N_2 band position, however, and the enhancements in strength were noted but not quantified. Here we attempt to quantify the extent of the enhancements as a function of the identity of the guest molecule and its relative concentration.

It is apparent from the intrinsic strengths (*A* values) of the N≡N stretching bands in Table I that the strength of the N_2 band depends critically on the identity of the second molecule in the sample. The N_2 stretching fundamental in ices containing ~5% CO, CH_4, O_2, or NH_3 has a strength that is similar that of pure N_2. In contrast, the presence of 5% H_2O or CO_2 produces significant enhancements in the strength of the N_2 feature, factors of about 10 and 100, respectively. In order to further understand these effects, we carried out a series of spectral measurements of ices having a wide variety of ratios of N_2 to CO, CH_4, O_2, NH_3, H_2O, and CO_2. The results of these experiments are summarized in Table II. The results based on the fringe technique are presented graphically in Fig. 3.

It is apparent from Table II and Fig. 3 that the presence of CO, CH_4, and O_2 in N_2-containing ices have little affect on the intrinsic strength of the N_2 band, even at large concentrations. In

contrast, the presence of NH_3, H_2O, or CO_2 cause the strength of the N_2 band to measurably increase as their concentration rises. The effect produced by NH_3 is moderate; substantial growth in N_2 band strength is not seen until the NH_3 concentration exceeds about 10% and the enhancement increases to a factor of slightly over 40 as the N_2/NH_3 ratio drops to 1. H_2O has a greater effect than NH_3. It produces measurable enhancement in the N_2 fundamental at concentrations as low as a few percent and causes increases in the N_2 band intensity greater than a factor of 80 in ices rich in H_2O.

The most dramatic effect, however, is produced by the presence of CO_2. Even at concentrations as low as 0.25%, the presence of CO_2 measurably enhances the strength of the N_2 fundamental, and at concentrations above 5% it enhances the N_2 fundamental by factors of hundreds. In very CO_2-rich ices, the enhancement exceeds a factor of 1000. It should be noted that the 2332.0 cm^{-1} band attributed to $^{18}O{=}C{=}O$ in the spectra of N_2-CO_2 mixtures (see also §4.2.2 and Fig. 2) is not included in the N_2 band areas reported in Tables I and II. All band intensities listed in these tables and displayed in Fig. 3 include *only* the absorption of the band at 2328.2 cm^{-1}. However, there is a certain ambiguity in the values reported in Table II in our samples with $N_2/CO_2 \leq 5$. Fig. 2 shows that the bands due to $^{18}O^{12}C^{16}O$ and N_2 begin to overlap and coalesce at high CO_2 concentrations. These two bands increase in strength together at lower concentrations (Fig. 2). As they begin to coalesce at $N_2/CO_2 = 5/1$, their relative proportions appear to be about $^1/_3$ to $^2/_3$ [21] and we assume they maintain this proportion at higher CO_2 concentrations. Therefore, the values in Table II for $N_2/CO_2 \leq 5$ are calculated assuming that $^2/_3$ of the combined band at high CO_2 concentrations is due to the N_2.

Two additional items are worthy of note. First, while our spectrometer is not very sensitive above 4000 cm^{-1}, we were occasionally able to detect the N_2 overtone band near 4656 cm^{-1}. In several samples having N_2/H_2O ratios between 10 and 20 we observed overtones having strengths of between $2.7x10^{-23}$ and $3.9x10^{-23}$ cm/molecule, values that are enhanced relative to those reported for pure N_2 (see [20]) by *at most* a factor 2, whereas the fundamentals in these samples are enhanced by factors of about 8. Similarly, the overtones seen in a few of our $N_2/CO_2 = 20/1$ and $N_2/CO_2 = 5/1$ samples yield strengths of a *maximum* of $4.2x10^{-22}$ and $1.4x10^{-21}$

cm/molecule, respectively. These correspond to enhancements of less than a factor of about 20 and 70 for the overtones, while the fundamentals are enhanced by factors of about 110 and 660, respectively. Thus, it appears that the N_2 overtone is less enhanced by the presence of H_2O and CO_2 than is the fundamental. Additional spectral measurements with higher signal to noise in the 4700-4600 cm^{-1} region will be needed to better quantify this observation, and for the remainder of this paper we will restrict ourselves to discussion of the N_2 fundamental.

Second, in a limited number of experiments we monitored the strength of the N_2 band as the samples were warmed to 20, 25, and 30 K. The H_2O- and CO_2-induced enhancements in the strength of the N_2 fundamental were seen to decrease slightly with warm up, the effect being less than 30% for CO_2 and perhaps as much as 50% for H_2O. Again, additional experiments will be required to better quantify this effect as a function of sample composition.

3.3 Isotopic Labeling

In order to gain a better understanding of the mechanisms responsible for the enhancement of the nitrogen fundamental in the presence of H_2O and CO_2, we carried out several experiments using isotopically-labeled N_2 and CO_2. When the nitrogen in the N_2-H_2O = 20/1 mixtures was replaced with isotopically-labeled $^{15}N_2$, the N≡N fundamental at 2328.2 cm^{-1} was observed to shift down to ~2250 cm^{-1} (4.444 μm) with essentially no change in strength (Fig. 4a,b and Table II), i.e., the same enhancements were seen when either $^{14}N_2$ or $^{15}N_2$ were used (enhancement factors of 8.9 ± 2.2 versus 6.1 ± 1.1, respectively). $^{15}N_2$-CO_2 mixtures demonstrated the same shift in the nitrogen band position, but in this case with a substantial reduction in the band's strength. For a $^{15}N_2/CO_2$ = 20/1 mixture, the N_2 stretching band decreases in strength by a factor of about 6 relative to an isotopically-normal N_2/CO_2 = 20/1 mixture (Fig. 4c,e and Table II), but is still enhanced relative to pure N_2 by a factor of about 18. The 2332 cm^{-1} band, which we earlier attributed to the $^{18}O{=}^{12}C$ asymmetric stretch of $^{18}O^{12}C^{16}O$, remains at 2332 cm^{-1} when $^{15}N_2$ is used, as expected. Finally, in N_2-$^{13}CO_2$ mixtures there is no change in the position of the 2328 cm^{-1} N≡N stretch, but its intensity diminishes. For an $N_2/^{13}CO_2$ = 20/1 mixture, the N_2 stretching band decreases by a factor of ~6 in strength

relative to an isotopically-normal N_2/CO_2 = 20/1 mixture (Fig. 4c,d and Table II), but is still enhanced relative to pure N_2 by a factor of about 18.

4. Discussion

4.1 Band Positions and Profiles

The relative invariance of the N_2 band profiles (Fig. 1) and strengths (Table II) make it clear that there is no strong interaction between N_2 and CO, CH_4, or O_2 in our samples. The broadening in the position of the N_2 feature in the presence of NH_3 and H_2O is probably due to hydrogen-bonding interactions. Such effects are commonly observed for other molecules frozen at these temperatures in H_2O-containing matrices [16,17]. The N_2-H_2O system has been previously studied by Andrews and Davis [10], who used Ar matrix-isolation techniques to demonstrate that N_2 interacts with hydrogen-bonding molecules in a way that suggests that an electronic structure readjustment in a monomeric complex occurs that results in a slightly stronger N≡N bond within the complex. This effect was observed to be the strongest in HF, but weaker hydrogen bonded complexes were observed for HCl and H_2O as well.

The position and profile of the N_2 band produced by N_2-CO_2 ices are not significantly different from those of pure N_2 and they provide little evidence for a strong N_2-CO_2 interaction. However, as we will see in the next section, the strength of the N_2 feature in these ices indicates otherwise.

4.2 Band Intensities

Again, CO, CH_4, and O_2 have little effect on the strength of the N_2 fundamental over a wide range of concentrations, while the presence of NH_3, H_2O, or CO_2 can result in a considerable increases in the band's intensity. The interactions whereby NH_3 and H_2O enhance the strength of the N_2 stretching band are thought to be fundamentally different from the CO_2 interaction.

4.2.1 The Intensity of the 2332.0 cm^{-1} N_2 Band in the Presence of NH_3 and H_2O

In N_2-H_2O mixtures rich in H_2O, the intensity of the 2328 cm^{-1} N_2 fundamental reaches a value of at least $A_{N2} \approx 1.4 \times 10^{-20}$ cm/molecule at N_2/H_2O = 1, i.e., almost 80 times greater than

for pure solid N_2 (see Table II and Figure 3). The enhancements produced by NH_3 are less dramatic, but still exceed a factor of 40 at high NH_3 concentrations. These N_2 band strength enhancements are probably the result of the same interactions that are producing band shifting [10] and broadening (see also Fig. 1), namely hydrogen-bonding interactions. These interactions should produce a far greater breaking of the symmetry of the N≡N stretching vibrations of nitrogen molecules near or complexed with NH_3 and H_2O than is produced by N_2 with only N_2 neighbors, resulting in greater infrared activation. Band strength enhancements mediated by hydrogen-bonding have been previously observed in a number of molecules frozen in H_2O-containing ices. For example, the intrinsic strengths of the infrared-active stretching modes of CO and CO_2 increase by factors of ~2 and 3, respectively, in H_2O-rich ices when compared to the same modes in pure ices [22,23]. Even more dramatically, it has long been known that the intrinsic strength of the 3250 cm^{-1} O-H stretching mode of H_2O in an H_2O-only ice is ~100 times greater than the same mode when H_2O is in the gas phase or frozen in argon [24]. In the case of the N_2-H_2O system, an enhancement by hydrogen-bonding interactions is already suggested by the observation from band position measurements that N_2 interacts with hydrogen bonding molecules [10]. Furthermore, the smaller enhancement produced by NH_3 compared to H_2O is consistent with this interpretation since the earlier band position work indicates that the strength of the interaction between HF, HCl, and H_2O qualitatively correlates with electron affinity [10].

4.2.2 The Intensity of the 2332.0 cm^{-1} N_2 Band in the Presence of CO_2

For N_2/CO_2= 5/1 mixtures, the intensity of the 2328 cm^{-1} band is over 600 times greater than that of pure N_2. Beyond $N_2/CO_2 = 5$, the intensity reaches a 'plateau' value of about 2.5×10^{-19} cm/molecule, although it becomes difficult to accurately determine the area of the 2328 cm^{-1} N_2 feature because the 2328 and 2332.0 cm^{-1} bands begin to seriously overlap (see Fig. 2 and §3.2). This overlap provides a clue to the CO_2 interaction causing the observed N_2 band strength enhancements. Since the band at 2332.0 cm^{-1} is due to the asymmetric stretch of $^{18}O^{12}C^{16}O$, one would expect it to grow, relative to the N_2 feature at 2328 cm^{-1}, with increasing CO_2 concentration.

However, Fig. 2 shows that this is not the case; the two bands remain fairly constant in strength relative to each other over a 40 fold change in N_2/CO_2 ratio. The 'expected' strength of the 2332.0 cm^{-1} $^{18}O^{12}C^{16}O$ band relative to the main $^{16}O^{12}C^{16}O$ band near 2348 cm^{-1} can be assessed measuring the 2348 and 2332 cm^{-1} band areas in the spectra of Ar-CO_2 mixtures (where no N_2 is present) or $^{15}N_2$-CO_2 mixtures where there is no confusion with the N_2 fundamental (see Fig. 4e). We find that the strength of the 2332.0 cm^{-1} $^{18}O^{12}C^{16}O$ band is near that which would be expected on the basis of the observed 2348 cm^{-1} CO_2 band for a wide range of N_2/CO_2 ratios. Thus, both the shift of the 2332 cm^{-1} $^{18}O^{12}C^{16}O$ band at high CO_2 concentrations and the 'lock step' fashion with which the strength of the 2328 cm^{-1} N_2 feature increases with CO_2 concentration suggest a interactive relationship between the N_2 fundamental and the $^{18}O^{12}C^{16}O$ band.

We suspect that the enhancement of the N_2 fundamental is related to resonant interaction of the 2328 cm^{-1} N_2 band with the nearby O=C asymmetric stretches of $^{18}O^{12}C^{16}O$ at 2332 cm^{-1} and, possibly, $^{16}O^{12}C^{16}O$ at 2348 cm^{-1}. The resonant nature of this interaction is suggested by the observation that the enhancement of the N_2 band decreases with increasing frequency difference ($\Delta\nu$) between the N≡N fundamental and the nearby CO_2 bands. For example, for 20/1 ices, an enhancement of a factor of ~100 is seen in normal N_2-CO_2 samples [$\Delta\nu(^{14}N_2,^{18}O^{12}C^{16}O) = 4$ cm^{-1}, $\Delta\nu(^{14}N_2,^{16}O^{12}C^{16}O) = 17$ cm^{-1}] relative to pure N_2, while the enhancement decreases to a factor of about 18 for both N_2-$^{13}CO_2$ samples [$\Delta\nu(^{14}N_2,^{16}O^{13}C^{16}O) = 46$ cm^{-1}] and $^{15}N_2$-CO_2 samples [$\Delta\nu(^{15}N_2,^{16}O^{12}C^{16}O) = 94$ cm^{-1}]. The fact that in samples with $N_2/CO_2 > 5$, the 2332 cm^{-1} $^{18}O^{12}C^{16}O$ band is seen to produce enhanced absorption (albeit more modest) that essentially matches step with the enhancement of the N_2 band is further suggestive of a resonant exchange of energy between N_2 molecules and adjacent CO_2 molecules. These observations are consistent with the results described by DiLella and Tevault [7] for N_2 ices containing $^{16}O^{12}C^{16}O$, $^{16}O^{12}C^{18}O$, and $^{18}O^{12}C^{18}O$, and they ascribe this behavior to an electrostatic mechanism whose behavior is similar to that of a Fermi resonance. Note that this behavior is very different from that seen in our N_2-H_2O experiments were there is essentially no difference in the enhancement factor between the $^{14}N_2$ and $^{15}N_2$ variants (see Table II).

Our concentration studies allow us to place some constraints on the nature of the N_2-CO_2 interaction. Assume for the moment that the observed N_2 absorption band in N_2-CO_2 ices is due to the superposition of absorption contributions from N_2 molecules having only N_2 neighbors ($A_{N2N2} = 1.8 \times 10^{-22}$ cm/molecule) plus 'enhanced' absorption contributions from N_2 molecules having a significant interaction with an adjacent CO_2 molecule ($A_{N2CO2} = 2.5 \times 10^{-19}$ cm/molecule). Using this simple "on-off" model in which a given N_2 molecule either is or is not enhanced, it is possible to use simple nearest-neighbor calculations of the type used to predict the fractional abundance of monomers, dimers, trimers, etc. in matrix-isolation studies [25] to calculate the expected enhancement of the A_{N2} value as a function of N_2/CO_2 ratio. The most favorable fit to the N_2/CO_2 concentration data is provided when it is assumed that each CO_2 in the sample can enhance at most two N_2 molecules (see Fig. 5). Since the resonant interaction involves the N_2 stretching fundamental and the CO_2 asymmetric stretching vibration, it is not entirely unexpected that the effect might be restricted to the N_2 molecules at the two ends of the CO_2 molecule. However, this simple model clearly deviates from our observations as the CO_2 concentration increases beyond $N_2/CO_2 < 5$, presumably because this simple model doesn't fully describing the interaction of N_2 with CO_2 multimers. Nonetheless, it appears that it is possible to explain the main facets of the observed enhancements using a simple model based on resonant interactions of the ends of the guest CO_2 molecules with their nearest N_2 neighbors.

5. Astrophysical Implications

Most of the material in dense interstellar dust clouds is at very low temperatures ($T < 50$ K). At these temperatures the majority of gas phase species condense out onto the dust grains in the form of mixed molecular ices [17]. Studies of the position and profile of the interstellar band near 2140 cm^{-1} (4.67 μm) due to CO in these ices show that they can be divided into two main types, those dominated by polar, H_2O-rich matrices and those dominated by apolar molecules like CO, CO_2, N_2, and O_2 [13,22,26]. The presence of N_2 in interstellar ices is supported by the observation that one of the best fits to the CO band position and profile in the apolar ices is

provided by a N_2:O_2:CO_2:CO = 1:5:$^1/_2$:1 mixture [13], a mixture having a composition similar to that expected for the apolar ices on the basis of time-dependent chemistry models [27].

A major fraction of the N_2 molecules in an N_2:O_2:CO_2:CO = 1:5:$^1/_2$:1 mixture should have at least one CO_2 neighbor and, as a result, the N_2 fundamental in such astrophysical ices is likely to be enhanced by factors of *hundreds* over that of pure nitrogen. This is good news for astronomers in that this is a sufficiently large enhancement that it raises the very real possibility that it may be possible to directly detect the N_2 in interstellar ices. On the other hand, it will be very difficult to derive interstellar N_2 column densities from any N_2 feature detected without first doing a thorough job of characterizing the other molecular components in the ice.

Closer to home, the enhancements described here may also play a significant role in the interpretation of the spectra of Pluto and Neptune's satellite Triton, both of which show evidence for surface ices that contain both CO_2 and abundant N_2 [12,28,29]. A more detailed discussion of the astrophysical implications of this work will appear elsewhere [30].

6. Conclusions

We have studied the position, profile, and strength of the N≡N fundamental stretch of N_2 in binary ice mixtures containing CO, CH_4, O_2, NH_3, H_2O, and CO_2. Mixtures of N_2 with NH_3, H_2O, or CO_2 produce significant enhancements in the strength of the 2328 cm^{-1} absorption feature relative to that observed for pure N_2 ices or mixtures of N_2 with O_2, CH_4, or CO.

In the case of NH_3 and H_2O, the N_2 band strength enhancement is probably the result of hydrogen-bonding interactions which produce a far greater breaking of the symmetry of the N≡N stretching vibrations of nitrogen molecules near NH_3 and H_2O than is produced by N_2 with only N_2 neighbors. The enhancement of the N_2 fundamental in the presence of CO_2 is probably related to resonant interaction of the 2328 cm^{-1} N_2 band with the nearby O=C asymmetric stretches of $^{18}O^{12}C^{16}O$ at 2332 cm^{-1} and $^{16}O^{12}C^{16}O$ at 2348 cm^{-1}.

These results may have significant implications for the interpretation of astronomical data of N_2-containing ices in dense molecular clouds in the interstellar medium and on the surfaces of planets and satellites in the outer Solar System.

Acknowledgments

This work was supported by NASA grants 344-37-44-01 (Origins of Solar Systems Program) and 344-38-12-04 (Exobiology Program). The authors are grateful for useful discussions with L. Allamandola, D. Cruikshank, E. Young, and P. Ehrenfruend, and excellent technical support from R. Walker.

References

[1] A.L. Smith, W.E. Keller and H.L. Johnston, Phys. Rev., 79 (1950) 728.

[2] H.W. Löwen, K.D. Bier and H.J. Jodl, J. Chem. Phys., 93 (1990) 8565-8575.

[3] G. Cardini, R. Righini, H.W. Löwen and H.J. Jodl, J. Chem. Phys., 96 (1992) 5703-5711.

[4] F. Legay and N. Legay-Sommaire, Chemical Physics, 206 (1996) 363-373.

[5] L. Fredin, B. Nelander and G. Ribbergård, J. Mol. Spect., 53 (1974) 410-416.

[6] B. Nelander, Chem. Phys. Letters, 42 (1976) 187-189.

[7] D.P. DiLella and D.E. Tevault, D. E., Chem. Phys. Lett., 126 (1986) 38-42.

[8] M. Falk, J. Chem. Phys., 86 (1987) 560-564.

[9] B.R. Carr, B.M. Chadwick, C.S. Edwards, D.A. Long, F.C. Warton, J. Molec. Struct., 62 (1980) 291-295.

[10] L. Andrews and S.R. Davis, J. Chem. Phys., 83 (1985) 4983-4989.

[11] L. Jin and K. Knorr, Phys. Rev. B, 47 (1993) 14142-14149.

[12] D.P. Cruikshank, T.L. Roush, T.C. Owen, E. Quirico, E. and C. de Bergh, in B. Schmitt et al. (Eds.), Solar System Ices, Kluwer Acad. Pub, Netherlands, 1998, pp. 655-684.

[13] J. Elsila, L.J. Allamandola and S.A. Sandford, Astrophysical Journal, 479 (1996) 818-838.

[14] L.J. Allamandola, S.A. Sandford and G. Valero, Icarus, 76 (1988) 225-252.

[15] D.M. Hudgins, S.A. Sandford and L.J. Allamandola, J. Phys. Chem., 98 (1994) 4243-4253.

[16] D.M. Hudgins, S.A. Sandford, L.J. Allamandola and A.G.G.M. Tielens, Astrophysical Journal Supplemental Series, 86 (1993) 713-870.

[17] S.A. Sandford and L.J. Allamandola, Astrophysical Journal, 417 (1993) 815-825.

[18] J.A. Roux, B.E. Wood, A.M. Smith and R.R. Plyler, Arnold Engineering Development Center Report, AEDC-TR-79-81, (1980).

[19] T.A. Scott, Phys. Rep., 27 (1976) 87-157.

[20] R.B. Bohn, S.A. Sandford, L.J. Allamandola and D.P. Cruikshank, Icarus, 111 (1994) 151-173.

[21] The $^1/_3$ proportion in the N_2/CO_2 = 5/1 ice is consistent with the expected strength of the 2332 cm^{-1} $^{18}O^{12}C^{16}O$ band relative to the 2340 cm^{-1} CO_2 fundamental based on the $^{18}O^{12}C^{16}O/^{18}O^{12}C^{16}O$ band area ratio seen in Ar-CO_2 ices.

[22] S.A. Sandford, L.J. Allamandola, A.G.G.M. Tielens and G. Valero, Astrophysical Journal, 329 (1988) 498-510.

[23] S.A. Sandford and L.J. Allamandola, Astrophysical Journal, 355 (1990) 357-372.

[24] L.J. Allamandola, in Galactic and Extragalactic Infrared Spectroscopy, M. Kessler & P. Phillips (Eds.), D. Reidel, Dordrecht, (1984) pp. 5-35.

[25] R.E. Behringer, J. Chem. Phys., 29 (1958) 537-539.

[26] A.G.G.M. Tielens, A.T. Tokunaga, T.R. Geballe and F. Baas, Astrophysical Journal, 381 (1991) 181-199.

[27] L.B. d'Hendecourt, L.J. Allamandola and J.M. Greenberg, Astronomy and Astrophysics, 152 (1985) 130-150.

[28] D.P. Cruikshank, T.L. Roush, T.C. Owen, T.R. Geballe, C. de Bergh, B. Schmitt, R.H. Brown and M. J. Bartholomew, Science, 261 (1993) 742-745.

[29] T.C. Owen, T.L. Roush, D.P. Cruikshank, J.L. Elliot, L.A. Young, C. de Bergh, B. Schmitt, T.R. Geballe, R.H. Brown and M.J. Bartholomew, Science, 261 (1993) 745-748.

[30] M.P. Bernstein, S.A. Sandford and L.J. Allamandola, Astrophysical Journal, in preparation.

Table I - Positions, FWHM, and Strengths of the N≡N Stretching Features in Fig. 1

Ice mixture	Position in cm^{-1} (μm)	FWHM (cm^{-1})	*A* value of N_2 from band areas (cm/molecule)[a]	*A* value of N_2 from fringes (cm/molecule)[a]
pure $^{14}N_2$	2328.2 (4.295)	1.5	---	$(1.8 \pm 0.3) \times 10^{-22}$ [b]
pure $^{15}N_2$	2250.6 (4.443)	1.8	---	$(1.6 \pm 0.1) \times 10^{-22}$ [b]
$N_2/CO = 25/1$	2328.2 (4.295)	1.6	$(2.9 \pm 0.8) \times 10^{-22}$	$(2.1 \pm 0.7) \times 10^{-22}$
$N_2/CH_4 = 20/1$	2327.9 (4.296)	1.3	$(3.3 \pm 0.3) \times 10^{-22}$	$(4.1 \pm 0.7) \times 10^{-22}$
$N_2/O_2 = 20/1$	2328.2 (4.295)	1.4	---	$(2.4 \pm 0.3) \times 10^{-22}$
$N_2/NH_3 = 22/1$	2328.2 (4.295)	2.0	$(5.5 \pm 1.2) \times 10^{-22}$	$(5.1 \pm 0.9) \times 10^{-22}$
$N_2/H_2O = 20/1$	2328.4 (4.295)	3.3	$(4.7 \pm 0.7) \times 10^{-21}$	$(1.6 \pm 0.4) \times 10^{-21}$
$N_2/CO_2 = 20/1$	2328.6 (4.294) 2332.0 (4.288)	1.4 1.4	$(2.7 \pm 0.2) \times 10^{-20}$ [c]	$(1.9 \pm 0.1) \times 10^{-20}$ [c]

a) Stated uncertainties represent the standard deviations of multiple measurements. *A* values used for the band area derivations and indices of refraction used for the fringe derivations are discussed in §2.3.

b) For comparison, Bohn et al. [15] report a value of $A_{N2} = (1.3 \pm 0.6) \times 10^{-22}$ cm/molecule.

c) Does not include any contribution from the area of the 2332.0 cm^{-1} band (see §3.2).

Table II - The Strength of the Infrared N≡N Stretching Feature as a Function of Guest Molecule Composition and Concentration

Ice Composition and Ratios	Fraction of Guest Molecule (%)	*A* value of N_2 from band areas (cm/molecule)[a]	*A* value of N_2 from fringes (cm/molecule)[a]
pure $^{14}N_2$	0.0	---	$(1.8 \pm 0.3) \times 10^{-22}$ [b]
pure $^{15}N_2$	0.0	---	$(1.6 \pm 0.1) \times 10^{-22}$ [b]
N_2/CO	% CO		
850	0.1	$(3.0 \pm 1.2) \times 10^{-22}$	$(1.6 \pm 0.2) \times 10^{-22}$
25	3.8	$(2.9 \pm 0.8) \times 10^{-22}$	$(2.1 \pm 0.7) \times 10^{-22}$
5.0	16.7	$(4.1 \pm 0.2) \times 10^{-22}$	$(4.2 \pm 0.3) \times 10^{-22}$
N_2/CH_4	% CH_4		
20	4.8	$(3.3 \pm 0.3) \times 10^{-22}$	$(4.1 \pm 0.7) \times 10^{-22}$
5.0	16.7	$(5.7) \times 10^{-22}$ [c]	$(7.8 \pm 0.1) \times 10^{-22}$
N_2/O_2	% O_2		
20	4.8	---	$(2.4 \pm 0.3) \times 10^{-22}$
5.0	16.7	---	$(5.4 \pm 1.6) \times 10^{-22}$
N_2/NH_3	% NH_3		
22	4.3	$(5.5 \pm 1.2) \times 10^{-22}$ [d]	$(5.1 \pm 0.9) \times 10^{-22}$
10.4	8.8	$(2.0 \pm 0.2) \times 10^{-21}$	$(1.6 \pm 0.1) \times 10^{-21}$
4.8	17.2	$(2.9 \pm 0.1) \times 10^{-21}$	$(2.6 \pm 0.3) \times 10^{-21}$
0.97	50.8	$(8.6 \pm 1.6) \times 10^{-21}$	$(8.0 \pm 0.2) \times 10^{-21}$
N_2/H_2O	% H_2O		
325	0.3	$(7.7 \pm 0.1) \times 10^{-22}$	$(2.0 \pm 0.1) \times 10^{-22}$
130	0.8	$(6.6 \pm 2.4) \times 10^{-22}$	$(3.3) \times 10^{-22}$ [c]
100	1.0	$(8.4 \pm 2.1) \times 10^{-22}$	$(4.0 \pm 0.8) \times 10^{-22}$
43	2.3	$(2.0 \pm 0.5) \times 10^{-21}$	$(9.5 \pm 1.3) \times 10^{-22}$

20	4.8	$(4.7 \pm 0.7) \times 10^{-21}$	$(1.6 \pm 0.4) \times 10^{-21}$
15.5	6.1	$(5.0) \times 10^{-21}$ [c]	$(1.5) \times 10^{-21}$ [c]
11.0	8.3	$(4.3 \pm 0.4) \times 10^{-21}$	---
5.0	16.7	$(7.8) \times 10^{-21}$ [c]	$(3.6) \times 10^{-21}$ [c]
1.35	42.6	$(1.8 \pm 0.4) \times 10^{-20}$	$(1.4 \pm 0.1) \times 10^{-20}$
1.0	50.0	$(3.6) \times 10^{-20}$ [c]	$(1.6 \pm 0.1) \times 10^{-20}$
0.10	90.9	$(4.3 \pm 0.8) \times 10^{-20}$	---

N_2/CO_2	% CO_2	(e)	(e)
400	0.25	$(1.8 \pm 0.2) \times 10^{-21}$	$(1.4 \pm 0.1) \times 10^{-21}$
200	0.5	$(3.2 \pm 0.1) \times 10^{-21}$	$(4.0 \pm 0.4) \times 10^{-21}$
75	1.3	$(8.9 \pm 1.3) \times 10^{-21}$	$(5.3 \pm 0.4) \times 10^{-21}$
20	4.8	$(2.7 \pm 0.2) \times 10^{-20}$	$(1.9 \pm 0.1) \times 10^{-20}$
10	9.1	$(6.6 \pm 0.3) \times 10^{-20}$	$(4.4 \pm 0.1) \times 10^{-20}$
5.0	16.7	$(1.6 \pm 0.4) \times 10^{-19}$	$(1.2) \times 10^{-19}$ [c]
3.6	21.7	$(2.5 \pm 0.3) \times 10^{-19}$	$(1.7) \times 10^{-19}$ [c]
3.0	25.0	$(3.4 \pm 0.1) \times 10^{-19}$	$(2.1 \pm 0.1) \times 10^{-19}$
2.55	28.2	$(3.6) \times 10^{-19}$ [c]	---
2.25	30.8	$(3.9 \pm 0.7) \times 10^{-20}$	$(2.7 \pm 0.1) \times 10^{-19}$ [c]
2.0	33.3	$(3.7 \pm 0.1) \times 10^{-19}$	$(2.2) \times 10^{-19}$ [c]

$N_2/^{13}CO_2$	% $^{13}CO_2$		
75	1.3	$(1.1 \pm 0.2) \times 10^{-21}$ [f]	$(1.3 \pm 0.3) \times 10^{-21}$
20	4.8	$(3.5 \pm 0.1) \times 10^{-21}$ [f]	$(3.2 \pm 0.1) \times 10^{-21}$
4	20	$(8.5 \pm 0.2) \times 10^{-21}$ [f]	$(6.6 \pm 0.1) \times 10^{-21}$

$^{15}N_2/CO_2$	% CO_2		
20	4.8	$(3.8 \pm 0.3) \times 10^{-21}$	$(3.2 \pm 0.4) \times 10^{-21}$

$^{15}N_2/H_2O$	% H_2O		
20	4.8	$(3.3 \pm 0.4) \times 10^{-21}$	$(1.1 \pm 0.2) \times 10^{-21}$
9	10	$(5.0 \pm 1.1) \times 10^{-21}$	$(3.7) \times 10^{-21}$ [c]

a) Stated uncertainties represent the standard deviations of multiple measurements. *A* values used for the band area derivations and indices of refraction used for the fringe derivations are discussed in §2.3.

b) This work. For comparison, Bohn et al. [15] report a value of $A_{N2} = (1.3 \pm 0.6) \times 10^{-22}$.

c) Result of a single measurement.

d) For our most dilute N_2:NH_3 = 22:1 samples we found that the value of A_{NH3}(1070 cm^{-1} band) = 1.7×10^{-17} cm/molecule provided very different results from those obtained using fringes. Study of a series of N_2-NH_3-CO samples, where the CO was used as a 'trace' band area standard, indicated that the *A* values of all the NH_3 bands fall off significantly as the NH_3 is diluted to N_2/NH_3 = 20/1 and beyond. For the N_2/NH_3 = 22/1 value we have scaled against the CO band area in an $N_2/NH_3/CO$ = 22/1/0.2 ice sample.

e) Does not include any contribution from the area of the 2332.0 cm^{-1} band (see §3.2).

f) Calculations assume $A^{13}CO_2$(2280 cm^{-1}) = 1.0×10^{-16} cm/molecule based on work done here.

Figure Captions

Fig. 1 - The 2338-2322 cm^{-1} (4.277-4.307 μm) infrared spectra of the N≡N stretching fundamental of (a) pure N_2, (b) N_2/CO = 25/1, (c) N_2/CH_4 = 20/1, (d) N_2/O_2 = 20/1, (e) N_2/NH_3 = 22/1, (f) N_2/H_2O = 20/1, and (g) N_2/CO_2 = 20/1 ices deposited and maintained at 12 K.

Fig. 2 - The 2338-2322 cm^{-1} (4.277-4.307 μm) infrared spectra of N_2/CO_2 ice samples deposited and maintained at 12 K. The N_2/CO_2 ratios of the samples are (a) 400/1, (b) 200/1, (c) 20/1, (d) 10/1, (e) 5/1, and (f) 2/1. The increasingly strong fall off to higher frequency as CO_2 concentration increases is due to the growth of the strong $^{16}O^{12}C^{16}O$ stretching fundamental near 2344 cm^{-1}.

Fig. 3 - The change in the intensity of the N≡N stretch near 2328.2 cm^{-1} (4.295 μm) as a function of the concentration of added CO (o), CH_4 (+), O_2 (×), NH_3 (Δ), H_2O (▲), and CO_2 (•). Note that the values plotted for the N_2-CO_2 ices represent only the contribution from the band near 2328 cm^{-1}, i.e., they do not include the area of 2332 cm^{-1} band. The dotted horizontal line near the bottom of the figure denotes the absorption strength of the 2328 cm^{-1} N_2 fundamental in pure nitrogen ices (Reference 20 and this work). All the values in this figure were determined using the interference fringe technique (see Table II).

Fig. 4 - The 2400-2200 cm^{-1} (4.17-4.55 μm) infrared spectra of the N≡N stretching fundamental for several normal and isotopically spiked samples deposited and maintained at 12 K. The samples are (a) N_2/H_2O= 20/1, (b) $^{15}N_2/H_2O$= 20/1, (c) N_2/CO_2 = 20/1, (d) $N_2/^{13}CO_2$ = 20/1, and (e) $^{15}N_2/CO_2$ = 20/1. The various spectra have been scaled by arbitrary amounts and the stronger bands in (c), (d), and (e) have been truncated for clarity.

Fig. 5 - A comparison of the observed N_2 band enhancement as a function of N_2/CO_2 ratio with predictions from a simple model based on nearest-neighbor considerations. The model assumes A_{N2} = 1.8x10^{-22} cm/molecule for all the N_2 molecules in the sample except those that are resonantly enhanced by an interaction with CO_2. Resonantly enhanced N_2 are all assumed to have A_{N2} = 2.5x10^{-19} cm/molecule. The theoretical curves correspond to different assumptions regarding how many N_2 molecules are enhanced by each CO_2. From the upper to lower curve they correspond to every CO_2 enhancing 6, 4, 2, and 1 neighboring N_2 molecule, respectively. It is clear that the best fit is provided when each CO_2 molecule is assumed to enhance two adjacent N_2 molecules.

Figure 1

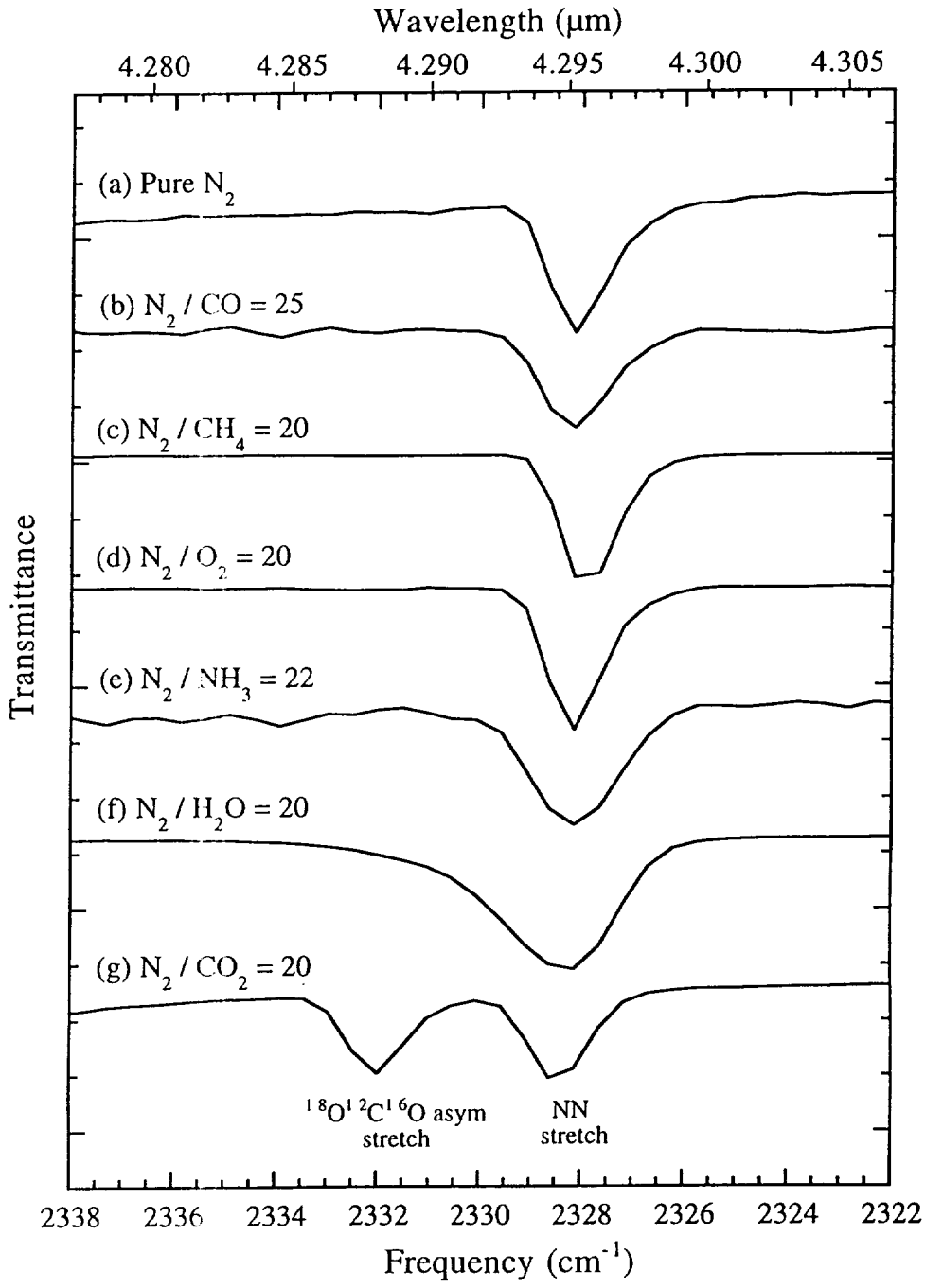
Wavelength (μm)
4.280
4.285
4.290
4.295
4.300
4.305
(a) Pure N_2
(b) N_2 / CO = 25
(c) N_2 / CH_4 = 20
(d) N_2 / O_2 = 20
(e) N_2 / NH_3 = 22
(f) N_2 / H_2O = 20
(g) N_2 / CO_2 = 20
Transmittance
$^{18}O^{12}C^{16}O$ asym stretch
NN stretch
2338
2336
2334
2332
2330
2328
2326
2324
2322
Frequency (cm^{-1})

Figure 2

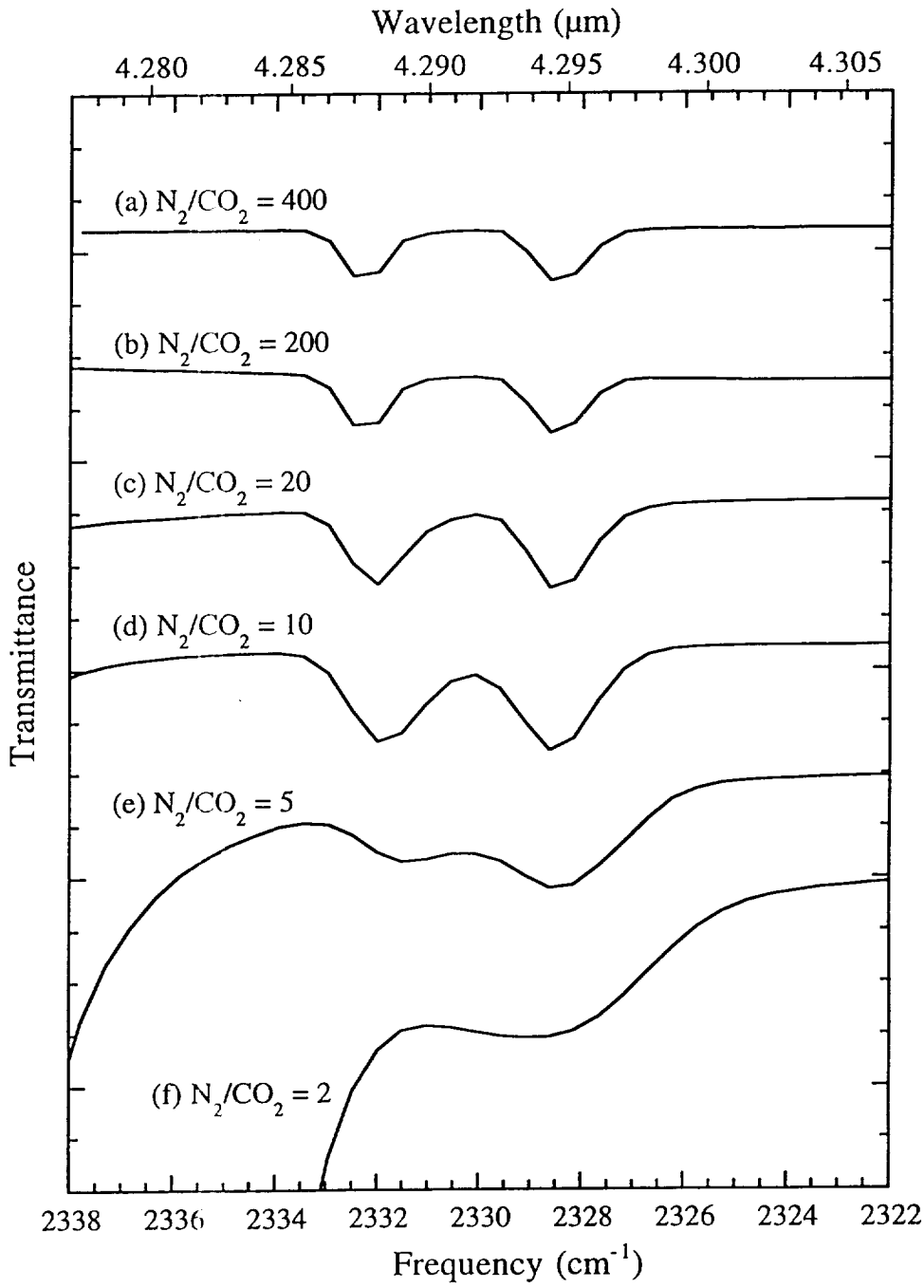
Wavelength (μm)
4.280
4.285
4.290
4.295
4.300
4.305
(a) $N_2/CO_2 = 400$
(b) $N_2/CO_2 = 200$
(c) $N_2/CO_2 = 20$
(d) $N_2/CO_2 = 10$
(e) $N_2/CO_2 = 5$
(f) $N_2/CO_2 = 2$
Transmittance
2338
2336
2334
2332
2330
2328
2326
2324
2322
Frequency (cm^{-1})

Figure 3

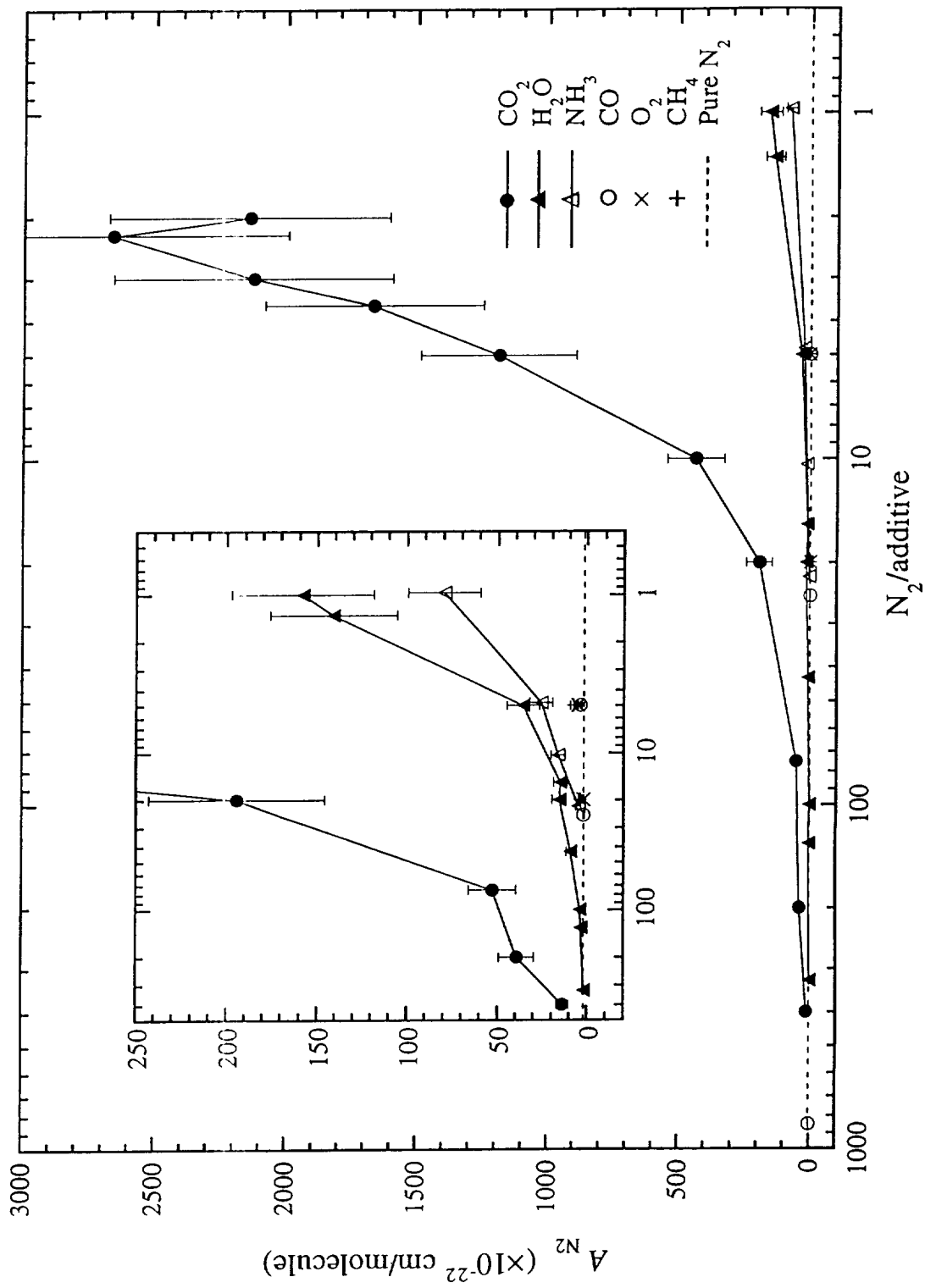

Figure 4

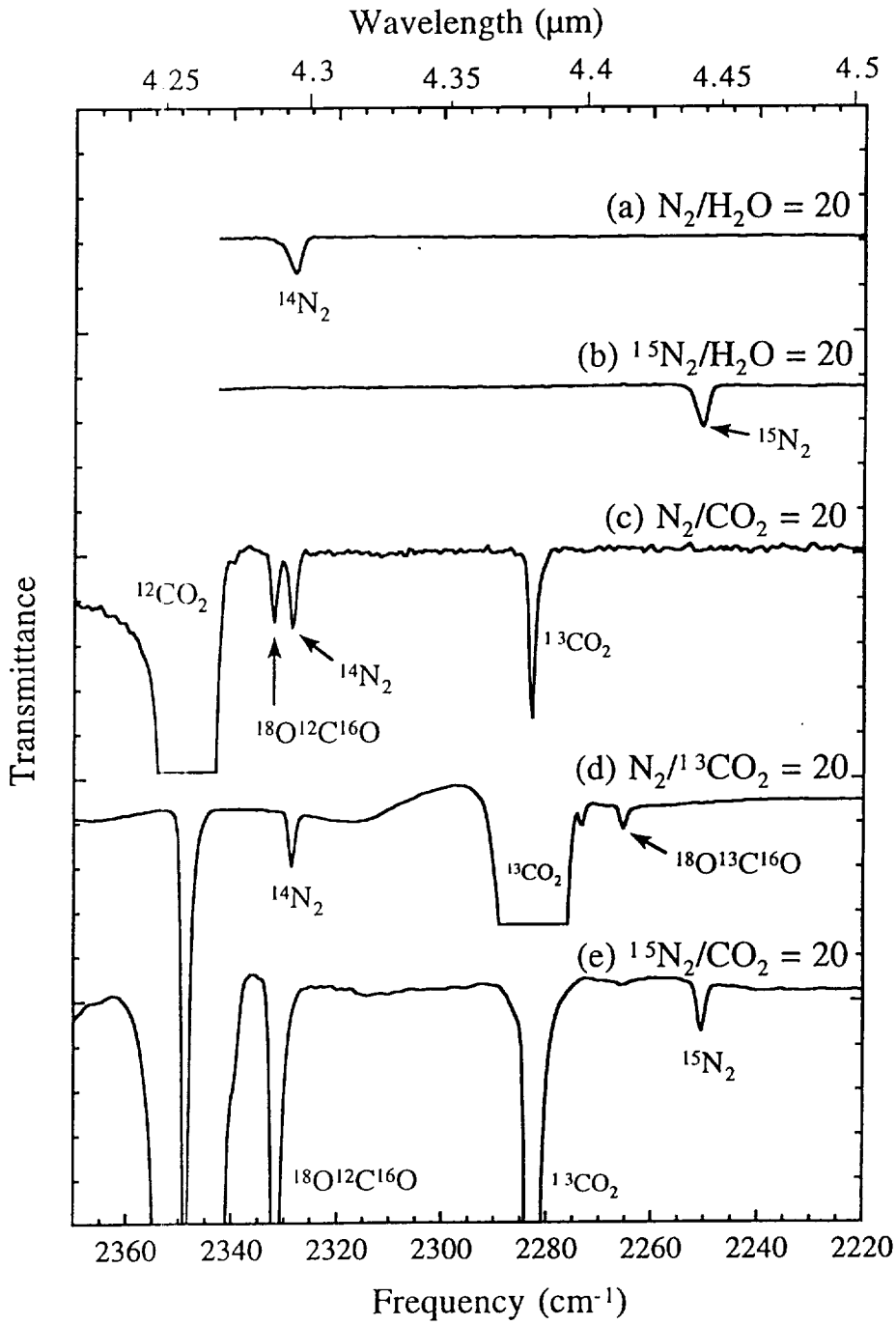
Wavelength (μm)
4.25
4.3
4.35
4.4
4.45
4.5
(a) $N_2/H_2O = 20$
$^{14}N_2$
(b) $^{15}N_2/H_2O = 20$
$^{15}N_2$
(c) $N_2/CO_2 = 20$
$^{12}CO_2$
$^{14}N_2$
$^{13}CO_2$
$^{18}O^{12}C^{16}O$
(d) $N_2/^{13}CO_2 = 20$
$^{14}N_2$
$^{13}CO_2$
$^{18}O^{13}C^{16}O$
(e) $^{15}N_2/CO_2 = 20$
$^{15}N_2$
$^{18}O^{12}C^{16}O$
$^{13}CO_2$
Transmittance
2360
2340
2320
2300
2280
2260
2240
2220
Frequency (cm^{-1})

Figure 5

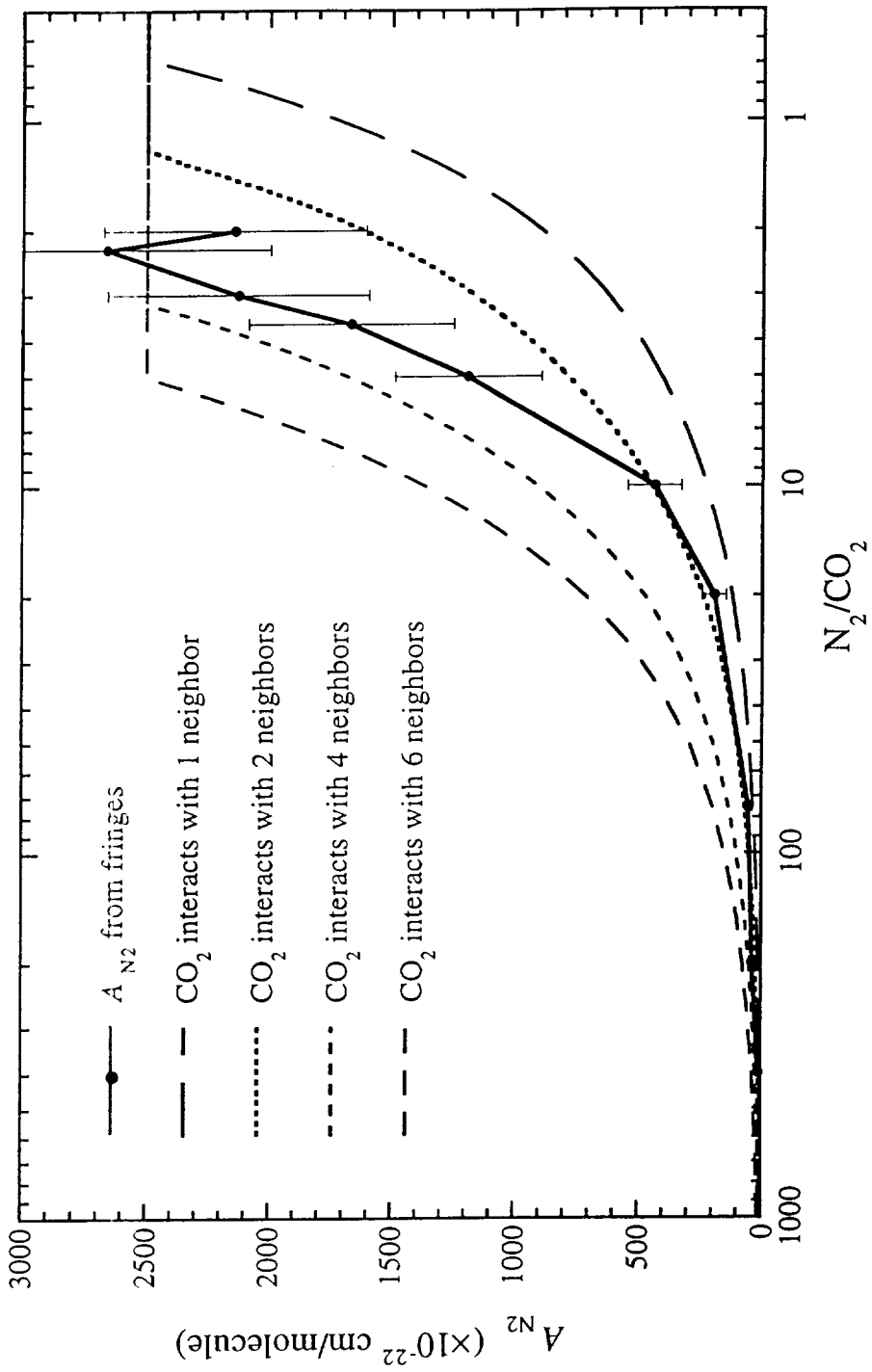
A_{N_2} ($\times 10^{-22}$ cm/molecule)
3000
2500
2000
1500
1000
500
0
1000
100
10
1
N_2/CO_2
A_{N2} from fringes
CO_2 interacts with 1 neighbor
CO_2 interacts with 2 neighbors
CO_2 interacts with 4 neighbors
CO_2 interacts with 6 neighbors